EPJ Web of Conferences **95**, 04036 (2015)
DOI: 10.1051/epjconf/ 20159504036

Rare B decays and processes with the ATLAS detector

Stefanos Leontsinis[1,2,a], on behalf of the ATLAS Collaboration

[1] *National Technical University of Athens*
[2] *Brookhaven National Laboratory*

Abstract. We present rare B decays and processes measured with the ATLAS detector. First, the associated production of vector boson + prompt J/ψ that is a key process for understanding of quarkonium production mechanisms, and second, the rare $B_s^0 \to \mu^+\mu^-$ decay, that due to its small branching fraction, is an excellent probe for physics beyond the standard model.

1 Introduction

The ATLAS detector is a multi-purpose detector [1][1] at the Large Hadron Collider (LHC) [2]. During 2011, ATLAS recorded 5.1 fb^{-1} of data on pp collisions at $\sqrt{s} = 7$ TeV. In these proceedings, we present two analyses, from the rich ATLAS B-physics program, performed with the 2011 data and focusing on the rare B decays and processes: the first measurement of the associated production of $W^{\pm}+$ prompt J/ψ in the $W^{\pm}(\to \mu^{\pm}\nu_{\mu}) + J/\psi(\to \mu^+\mu^-)$ channel [3], and the search for the $B_s^0 \to \mu^+\mu^-$ rare decay [4].

1.1 The ATLAS detector

The inner detector (ID) of ATLAS, surrounded by a superconducting solenoid producing 2 T magnetic field, provides tracking information for charged particles with $|\eta| < 2.5$. The muon spectrometer (MS) covers up to $|\eta| = 2.7$ and, in combination with the ID, can reconstruct muons with $p_{\mathrm{T}} \geq 2.5$ GeV with resolution $\sigma(p_{\mathrm{T}})/p_{\mathrm{T}}$ better than 3% (in the momentum range used in this analysis). Muon detectors are also used to trigger on high transverse momentum muons.

During 2012, ATLAS recorded more than 21 fb^{-1} of data on pp collisions at $\sqrt{s} = 8$ TeV.

2 First measurement of associated vector boson plus prompt charmonium production

The associated production of the $W^{\pm}$ boson and prompt J/ψ is a key process in understanding the colour singlet (CS) and colour octet (CO) models [5, 6]. It has different initial condition compared to

[a] e-mail: stefanos.leontsinis@cern.ch

[1] ATLAS uses a right-handed coordinate system with its origin at the nominal interaction point (IP) in the centre of the detector and the z-axis along the beam pipe. The x-axis points from the IP to the centre of the LHC, and the y-axis points upward. Cylindrical coordinates (r, ϕ) are used in the transverse plane, ϕ being the azimuthal angle around the beam pipe. The pseudorapidity is defined in terms of the polar angle θ as $\eta = -\ln\tan(\theta/2)$. The distance ΔR in $\eta - \phi$ space is defined as $\Delta R = \sqrt{\Delta\eta^2 + \Delta\phi^2}$.

the inclusive J/ψ production, making it ideal for testing the contributions of CS and CO processes in the J/ψ composition. Furthermore, the associated production of $W^{\pm}+J/\psi$ includes two processes: single parton scattering (SPS) and double parton scattering (DPS), where the $W^{\pm}$ and the J/ψ are produced from the same or two different pairs of partons, respectively.

2.1 Event selection

The J/ψ is reconstructed requiring muons to have $p_{\mathrm{T}} > 3.5\,(2.5)\,\mathrm{GeV}$ for $|\eta| < 1.3\,(> 1.3)$, both to lie within the angular acceptance of both the ID and MS ($|\eta| < 2.5$), to originate at a common point and at least one muon with $p_{\mathrm{T}} > 4\,\mathrm{GeV}$. The invariant mass of the dimuon system must be within $2.5 < m_{\mu^+\mu^-} < 3.5\,\mathrm{GeV}$. To establish high acceptance and efficiency, the transverse momentum of the J/ψ is required to be $p_{\mathrm{T}}^{J/\psi} > 8.5\,\mathrm{GeV}$ and its rapidity $|y^{J/\psi}| < 2.1$. Finally, an upper cut of $p_{\mathrm{T}}^{J/\psi} < 30\,\mathrm{GeV}$ is applied to improve the signal to background ratio.

The candidate muon coming from the $W^{\pm}$ decay is required to match the muon fired the high p_{T} single muon trigger, and to have $p_{\mathrm{T}} > 25\,\mathrm{GeV}$ and $|\eta| < 2.4$. The transverse momentum imbalance measured in the detector must satisfy $E_{\mathrm{T}}^{\mathrm{miss}} > 20\,\mathrm{GeV}$, and the transverse mass[2] of the $W^{\pm}$ needs to be $m_{\mathrm{T}}^{W} > 40\,\mathrm{GeV}$.

In order to reject Z + jet events, mimicking the final state, events having two oppositely charged muons with invariant mass within 10 GeV of the Z boson mass are rejected. 149 events are left after the application of the selections (see Figure 1a).

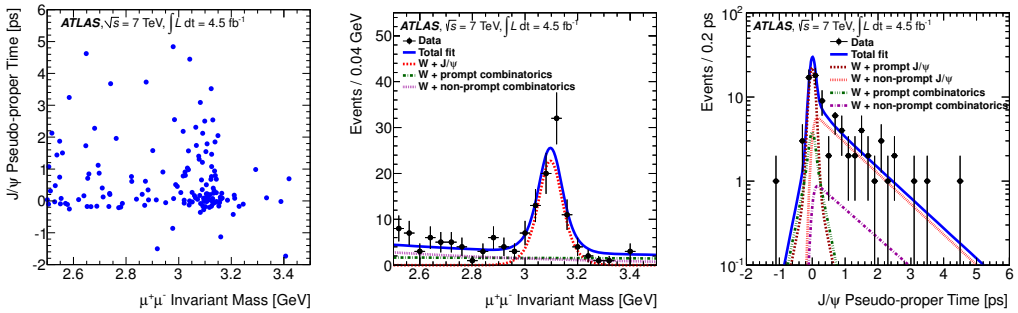

(a) (b) (c)

Figure 1: (a) Two-dimensional plot of $W^{\pm}+J/\psi$ candidates in J/ψ pseudo-proper time versus $\mu^+\mu^-$ invariant mass. Projections in invariant mass (b) and pseudo-proper time (c) of the two-dimensional mass-pseudo-proper time fit used to extract the prompt J/ψ candidates in the full rapidity region ($|y_{J/\psi}| < 2.1$). The pseudo-proper time distribution is shown for the J/ψ mass peak region ($3.0 < m(\mu^+\mu^-) < 3.2\,\mathrm{GeV}$).

J/ψ signal events are separated from combinatorial background events, and the prompt J/ψ signal is separated from the non-prompt signal, by a 2D maximum likelihood fit, performed in the mass (Figure 1b) and pseudo-proper time (Figure 1c) observables. We find $29.2^{+7.5}_{-6.5}$ $W^{\pm}+$ prompt J/ψ

[2] $m_{\mathrm{T}}(W) \equiv \sqrt{2 p_{\mathrm{T}} E_{\mathrm{T}}^{\mathrm{miss}} (1 - \cos(\phi^{\mu} - \phi^{\nu_{\mu}}))}$

events with a statistical significance of 5.1σ. Pileup events (events produced in different proton-proton collisions in the same bunch crossing) are estimated to be 1.8 ± 0.2. After the fit is performed, the extracted prompt J/ψ yield is used to produce per event weights, using the sPlot tool [7]. Applying these weights to the dataset we get the m_{T}^{W} distribution weighted according to events that are associated with prompt J/ψ mesons. Fitting the weighted m_{T}^{W} distribution (Figure 2a) with a multijet template plus the signal $W^{\pm}$ template (Figure 2b), the $W^{\pm}$ signal hypothesis is strongly supported and an estimation of 0.1 ± 4.6 of multijet events is calculated.

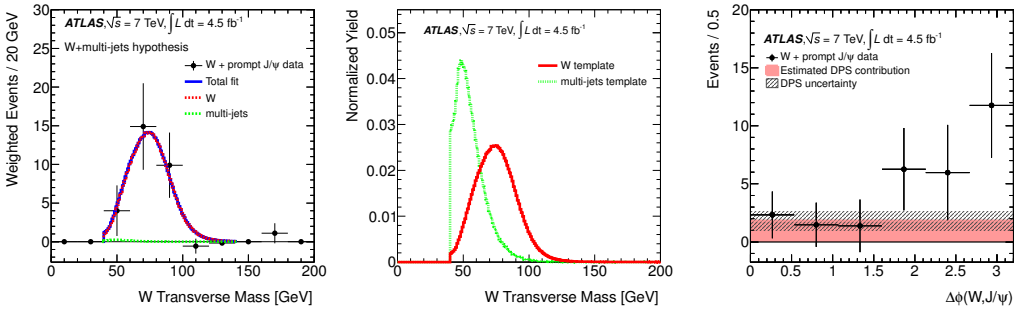

(a) (b) (c)

Figure 2: (a) sPlot-weighted $W^{\pm}$ boson transverse mass distribution for $W^{\pm}$ boson and multi-jet components. (b) Unit-normalized templates for $W^{\pm}$ boson transverse mass $m_{\mathrm{T}}(W)$ for multijet background and $W^{\pm}$ signal. (c) The sPlot-weighted azimuthal angle between the $W^{\pm}$ and the J/ψ for $W^{\pm}+$ prompt J/ψ candidates.

2.2 Double parton scattering

In a fraction of the selected events, the $W^{\pm}$ and the J/ψ may have occured from the scattering of two different pairs of partons in the same proton-proton collision. The probability that an extra J/ψ is produced in addition to the production of the $W^{\pm}$ can be formulated as $P_{J/\psi|W^{\pm}} = \sigma_{J/\psi}/\sigma_{\mathrm{eff}}$, with σ_{eff} being the effective cross section parameter, measured by ATLAS using $W^{\pm}(\rightarrow l\nu) + 2$ jets events to be $\sigma_{\mathrm{eff}} = 15 \pm 3(\mathrm{stat.})^{+5}_{-3}(\mathrm{syst.})\,\mathrm{mb}$ [8]. Comparing the result for the σ_{eff} with other measurements at Tevatron and SPS indicates that its value is not strongly dependent of the process and the centre of mass energy. ATLAS measurement of the inclusive prompt J/ψ production [9] is used for computing the $\sigma_{J/\psi}$, corrected for the fiducial phase space of this analysis. The estimation of the total number of DPS events is 10.8 ± 4.2.

The events coming from DPS are expected to be distributed uniformly along the azimuthal angle between the $W^{\pm}$ and the J/ψ, because the two interactions are assumed to be independent. Figure 2c shows the sPlot-weighted $\Delta\phi(W, J/\psi)$ distribution and indicates the SPS component (peaking at π) and DPS being a large fraction of the total statistics ($\approx 40\%$).

2.3 Cross section measurements

ATLAS collaboration measured the cross-section ratio of $W^{\pm} + J/\psi$ to inclusive $W^{\pm}$ (Figure 3a). The fiducial cross-section ratio of $W^{\pm}+$ prompt J/ψ relative to inclusive $W^{\pm}$ is measured to

be $R^{\mathrm{fid}}_{J/\psi} = (51 \pm 13(\mathrm{stat.}) \pm 4(\mathrm{syst.})) \times 10^{-8}$. The acceptance-corrected observed ratio is $R^{\mathrm{incl}}_{J/\psi} = \left(126 \pm 32(\mathrm{stat.}) \pm 9(\mathrm{syst.})^{+41}_{-25}\right) \times 10^{-8}$ with the last uncertainty representing variations to the unknown spin-alignment. Subtracting the DPS contribution we extract the SPS rate $R^{\mathrm{DPS\ sub}}_{J/\psi} = \left(78 \pm 32(\mathrm{stat.}) \pm 22(\mathrm{syst.})^{+41}_{-25}\right) \times 10^{-8}$. The last bin also presents LO colour-singlet and NLO colour-octet calculations for SPS production [10, 11].

Figure 3b shows the differential cross section ratio $\mathrm{d}R^{\mathrm{incl}}_{J/\psi}/\mathrm{d}p_{\mathrm{T}}$ as a function of the J/ψ transverse momentum. The DPS contribution is overlaid to the data and the measurement suggests a large SPS contribution in the low $p_{\mathrm{T}}^{J/\psi}$ bin.

Run II data will allow us to perform measurements of the relative fraction of SPS and DPS production. In addition, the $W^{\pm} + J/\psi$ channel is also used for studying the Higgs decays to charmonia and physics beyond the standard model (SM) [12].

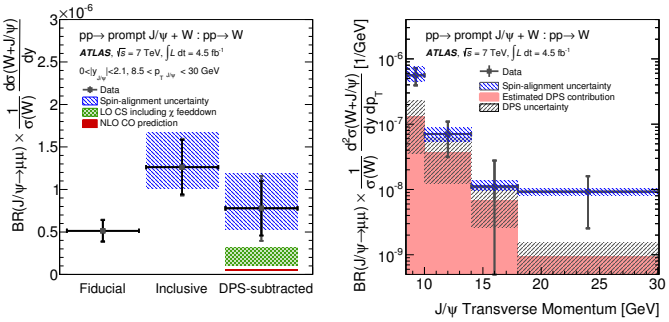

(a) (b)

Figure 3: (a) The $W^{\pm}+$ prompt J/ψ production differential cross-section ratio in the J/ψ fiducial region (Fiducial), after correction for J/ψ acceptance (Inclusive), and after subtraction of the double parton scattering component (DPS-subtracted). (b) The inclusive (SPS+DPS) cross-section ratio $\mathrm{d}R^{\mathrm{inl}}_{J/\psi}/\mathrm{d}p_{\mathrm{T}}$ as a function of $p_{\mathrm{T}}^{J/\psi}$.

3 Search for $B_s \to \mu^+\mu^-$ rare decay

The $B^0_s \to \mu^+\mu^-$ decay is a flavour changing neutral current process and the SM predicts a very small branching fraction, $(3.23 \pm 0.27) \times 10^{-9}$ [13], for this decay. This small branching fraction makes this channel very attractive for searching for new physics that may increase the branching fraction. The CMS and LHCb collaborations measured this branching fraction, using the full dataset collected during 2011 and 2012 with $\sqrt{s} = 7$ and 8 TeV, respectively, and found it to be consistent with the SM predictions [14, 15]. ATLAS updated its first analysis [16] and extended the search for the $B^0_s \to \mu^+\mu^-$ to the full 2011 dataset.

The $B^0_s \to \mu^+\mu^-$ branching fraction is measured with respect to the reference channel $B^{\pm} \to J/\psi K^{\pm} \to \mu^+\mu^- K^{\pm}$ in order to minimise the systematic uncertainties in the evaluation of the efficiencies and acceptances, without increasing the statistical uncertainties. The branching fraction can be written as

$$\mathscr{B}(B_s^0 \to \mu^+\mu^-) = \mathscr{B}(B^\pm \to J/\psi K^\pm \to \mu^+\mu^- K^\pm) \times \frac{f_u}{f_s} \times \frac{N_{\mu^+\mu^-}}{N_{J/\psi K^\pm}} \times \frac{A_{J/\psi K^\pm}}{A_{\mu^+\mu^-}} \frac{\varepsilon_{J/\psi K^\pm}}{\varepsilon_{\mu^+\mu^-}}, \quad (1)$$

where the $B^\pm \to J/\psi K^\pm \to \mu^+\mu^- K^\pm$ branching fraction and the relative b-quark hadronisation probability, f_u/f_s, of $B^\pm$ and B_s^0 are taken from previous measurements [17, 18]. The acceptance times efficiency ratio is evaluated using Monte Carlo (MC) samples, after the application of generator level and data driven corrections. The yield of the reference channel ($N_{J/\psi K^\pm}$) is extracted by performing an unbinned maximum likelihood fit in mass and mass resolution.

A blind analysis was performed where the data in the di-muon invariant mass region 5066 to 5666 MeV were removed from the analysis (the full region being $4766 - 5966$ MeV) until the procedures for event selection, signal and limit extractions were completely defined. The blinding of the invariant mass spectrum creates two regions: the sidebands (defined as $4766 - 5066$ MeV and $5666 - 5966$ MeV) and the signal region ($5066 - 5666$ MeV).

3.1 Event and signal selections

For the reference channel, we require the J/ψ mass to be within $2915 < m_{J/\psi} < 3175$ MeV. Tracks are required to have $|\eta| < 2.5$ and $p_{\mathrm{T}} > 4(2.5)$ GeV for muon (kaon) candidates. All B candidates are required to satisfy $p_{\mathrm{T}}^B > 8$ GeV and $|\eta^B| < 2.5$.

The signal to background discrimination is done using 13 variables in a multivariate classifier. The Boosted Decision Tree (BDT) algorithm found to be the best performing. Distributions from simulated $b\bar{b} \to \mu^+\mu^- X$ events are compared to sideband data (see Figure 4a), with the good agreement between data and simulation allowing the MC to be used for the training of the multivariate classifiers.

The 2D optimisation on the BDT output variable and the signal region width aims in obtaining the best sensitivity to the signal. It is performed by maximising the estimator of the separation power of the classifier $\mathscr{P} = \varepsilon/(1+\sqrt{B})$, where ε is the signal efficiency and B the number of background events selected.

Figure 4b shows the distributions of the chosen BDT output variable for signal MC events and mass sideband data.

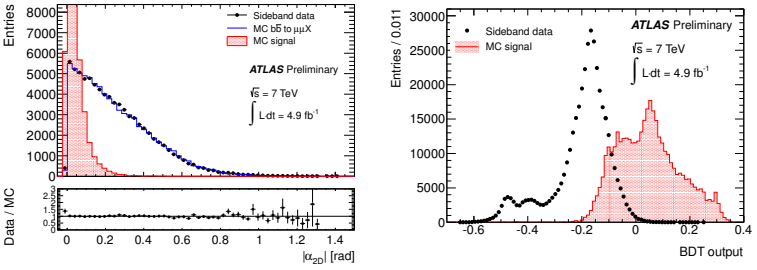

(a) (b)

Figure 4: (a) Comparisons between sideband data (black dots) and $b\bar{b} \to \mu^+\mu^- X$ MC events (blue solid histogram) for the $\alpha_{2\mathrm{D}}$[3] variable. The signal (red-filled solid histogram) is shown for shape comparison. The lower graph shows the data/MC ratio. (b) Distributions of the selected BDT for signal MC events and mass sideband data.

The reference channel yield $N_{J/\psi K^{\pm}}$ is determined from a multi-dimensional unbinned extended maximum likelihood fit to the distribution of the invariant-mass $m_{\mu^+\mu^-K^{\pm}}$ of the $\mu^+\mu^-K^{\pm}$ system (see Figure 5a) and its event-by-event uncertainty $\delta m_{\mu^+\mu^-K^{\pm}}$ (see Figure 5b).

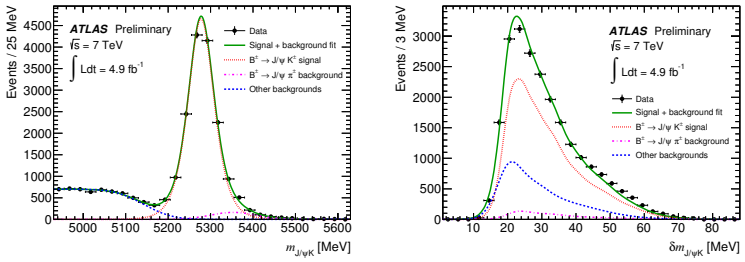

(a) (b)

Figure 5: (a) $m_{\mu^+\mu^-K^{\pm}}$ invariant mass spectrum and (b) $\delta_{\mu^+\mu^-K^{\pm}}$ mass uncertainty distribution (right) from even-numbered events passing all selection cuts. The results from the unbinned maximum likelihood fit are overlaid. The solid green curve is the total fit projection on top of the binned data distribution (black circles). The dotted red curve is the $B^{\pm} \to J/\psi K^{\pm}$ signal component, the dash-dotted magenta curve is the background from $B^{\pm} \to J/\psi\pi^{\pm}$ decays, and the dashed blue curve corresponds to the sum of the partially reconstructed B decays background and the combinatorial background components.

3.2 Branching fraction limit extraction

After determining all the ingredients of the equation 1, the $\mu^+\mu^-$ spectrum is unblinded and 6 events are counted in the signal region (see Figure 6a). Figure 6b shows the behaviour of the observed CL_s for different tested values of the $\mathscr{B}(B_s^0 \to \mu^+\mu^-)$. The observed limit is $\mathscr{B}(B_s^0 \to \mu^+\mu^-) < 1.5(1.2) \times 10^{-8}$ at 95% (90%) CL.

4 Conclusions

ATLAS has a rich B-physics program which includes indirect physics searches for new physics, like the measurement of the branching fraction of the rare $B_s^0 \to \mu^+\mu^-$ decay, and measurement of rare processes, like the production of the vector boson in association with prompt charmonium. Using the 2011 dataset of pp collisions at $\sqrt{s} = 7\,\text{TeV}$, we searched for the $B_s^0 \to \mu^+\mu^-$ decay and set a limit on its branching fraction (1.5×10^{-8} at 95%), and measured for the first time the cross section ratio of the associated production of $W^{\pm}$ and prompt J/ψ to inclusive $W^{\pm}$ production.

Acknowledgements

This research has been co-financed by the European Union (European Social Fund - ESF) and Greek national funds through the Operational Program "Education and Lifelong Learning" of the National Strategic Reference Framework (NSRF) - Research Funding Program: **THALES**. Investing in knowledge society through the European Social Fund.

[3] Absolute value of the angle in the transverse plane between $\Delta\vec{x} = \vec{x}_{\text{SV}} - \vec{x}_{\text{PV}}$ and $\vec{p}^{B}$.

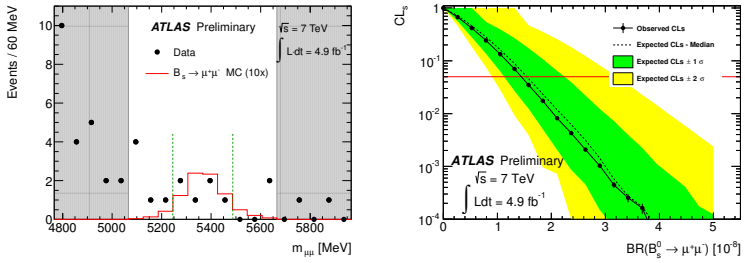

(a) (b)

Figure 6: (a) Invariant-mass distributions of selected candidates in data (dots). The plot also indicates the signal (continuous line) as predicted by MC assuming $\mathscr{B}(B_s^0 \to \mu^+\mu^-) = 3.5 \times 10^{-8}$ (scaled by a factor 10), the signal region (two dashed vertical lines) corresponding to the optimised Δm cut and the sidebands used in the analysis (grey areas). The expected number of $B_s^0 \to \mu^+\mu^-$ signal in the signal region is 1.7 ± 0.2 events. The expected background yield per bin in the signal region is 1.7 events. (b) Observed CL_s (circles) as a function of $\mathscr{B}(B_s^0 \to \mu^+\mu^-)$. The 95% CL limit is indicated by the horizontal (red) line. The dark (green) and light (yellow) bands correspond to the $\pm 1\sigma$ and $\pm 2\sigma$ ranges of the background-only pseudo-experiments with the median of the expected CL_s given by the dashed line.

References

[1] ATLAS Collaboration, JINST, **3** S08003 (2008)
[2] L. Evans and P. Bryant (editors), JINST, **3** S08001 (2008)
[3] ATLAS Collaboration, JHEP, **04**, 172 (2014) [arXiv:1401.2831]
[4] ATLAS Collaborations, ATLAS-CONF-2013-076, https://cds.cern.ch/record/1562934
[5] Quarkonium Working Group, N. Brambilla et al., Heavy Quarkonium Physics [arXiv:hep-ph/0412158]
[6] N. Brambilla et al., Eur. Phys. J. **C71**, 1534 (2011) [arXiv:1010.5827]
[7] M. Pivk and F. R. Le Diberder, Nucl. Instrum. Meth. A **555**, 356-369 (2005) [arXiv:hep-ph/0402083]
[8] ATLAS Collaboration, New J. Phys. **15**, 033038 (2013) [arXiv:1301.6872]
[9] ATLAS Collaboration, Nucl. Phys. B **850**, 387-444 (2011) [arXiv:1104.3038]
[10] J.P. Lansberg and C. Lorce, Phys. Lett. B **726**, 218-222 (2013) [arXiv:1303.5327]
[11] G. Li et al., Phys. Rev. D **83**, 014001 (2011) [arXiv:1012.3798]
[12] J. D. Clarke et al., JHEP **02**, 123 (2014) [arXiv:1310.8042]
[13] A. J. Buras, Girrbach, D. Guadagnoli, and G. Isidori, Eur. Phys. J. **C72** 2172 (2012) [arXiv:1208.0934]
[14] LHCb Collaboration, R. Aaij et al., Phys. Rev. Lett. **111**, 101805 (2013) [arXiv:1307.5024]
[15] CMS Collaboration, Phys. Rev. Lett. **111**, 101804 (2013) [arXiv:1307.5025]
[16] ATLAS Collaborations, Phys.Lett. B **713**, 387-407 (2012) [arXiv:1204.0735]
[17] Particle Data Group Collaboration, J. Beringer et al., Phys.Rev. **D86**, 010001 (2012)
[18] LHCb Collaboration, R. Aaij et al., JHEP **1304**, 001 (2013) [arXiv:1301.5286]